#### **ORIGINAL PAPER**



# Sustained inactivation of the Polycomb PRC1 complex induces DNA repair defects and genomic instability in epigenetic tumors

Chetan C. Rawal<sup>1</sup> · Vincent Loubiere<sup>2,3</sup> · Nadejda L. Butova<sup>1</sup> · Juliette Gracia<sup>2</sup> · Victoria Parreno<sup>2</sup> · Chiara Merigliano<sup>1</sup> · Anne-Marie Martinez<sup>2</sup> · Giacomo Cavalli<sup>2</sup> · Irene Chiolo<sup>1</sup>

Accepted: 27 May 2024 / Published online: 18 June 2024 © The Author(s) 2024

#### **Abstract**

Cancer initiation and progression are typically associated with the accumulation of driver mutations and genomic instability. However, recent studies demonstrated that cancer can also be driven purely by epigenetic alterations, without driver mutations. Specifically, a 24-h transient downregulation of *polyhomeotic* (*ph*-KD), a core component of the Polycomb complex PRC1, is sufficient to induce epigenetically initiated cancers (EICs) in *Drosophila*, which are proficient in DNA repair and characterized by a stable genome. Whether genomic instability eventually occurs when PRC1 downregulation is performed for extended periods of time remains unclear. Here, we show that prolonged depletion of PH, which mimics cancer initiating events, results in broad dysregulation of DNA replication and repair genes, along with the accumulation of DNA breaks, defective repair, and widespread genomic instability in the cancer tissue. A broad misregulation of H2AK118 ubiquitylation and to a lesser extent of H3K27 trimethylation also occurs and might contribute to these phenotypes. Together, this study supports a model where DNA repair and replication defects accumulate during the tumorigenic transformation epigenetically induced by PRC1 loss, resulting in genomic instability and cancer progression.

Keywords Epigenetically initiated cancers · Polycomb complex · Double-strand break repair · Genomic instability

### Introduction

The tumorigenic process is typically associated with DNA damage defects and genomic instability (Hopkins et al. 2022). However, recent studies established that cancer can

Chetan C. Rawal and Vincent Loubiere have contributed equally to this work.

- Anne-Marie Martinez anne-marie.martinez@igh.cnrs.fr
- ☐ Giacomo Cavalli giacomo.cavalli@igh.cnrs.fr
- ☐ Irene Chiolo chiolo@usc.edu
- Department of Molecular and Computational Biology, University of Southern California, 1050 Childs Way, Los Angeles, CA 90089, USA
- Institute of Human Genetics, CNRS, University of Montpellier, Montpellier, France
- Research Institute of Molecular Pathology, Vienna BioCenter, Vienna, Austria

also be induced purely by epigenetic changes initiated by the transient loss of the transcriptionally repressive Polycomb PRC1 complex (Parreno et al. 2024). Polycomb Group (PcG) proteins are grouped in two main classes of complexes called Polycomb Repressive Complex 1 and 2 (PRC1 and PRC2) (Levine et al. 2002; Kassis et al. 2017; Schuettengruber et al. 2017). Drosophila PRC1, which is composed of PH, PC, PSC, and SCE subunits, is primarily responsible for H2AK118 ubiquitylation (H2AK118ub, corresponding to H2AK119ub in mammals) (Barbour et al. 2020; Parreno et al. 2022), whereas PRC2 mediates H3K27 trimethylation (H3K27me3) (Holoch and Margueron 2017). PRC1 and PRC2 are also highly interdependent, given that PRC1 binds to H3K27me3 while PRC2 associates with H2AK118ub (Blackledge et al. 2014; Cooper et al. 2016, Kasinath et al. 2021). This enables cooperative binding of the two complexes to the same sites and codependency in the establishment of the respective marks on chromatin (Cooper et al. 2016; Barbour et al. 2020, Tamburri et al. 2020). While PRC1 and PRC2 form several redundant subcomplexes in mammalian cells (Parreno et al. 2022, Potter et al. 2023), Drosophila Polycomb complexes comprise a reduced



number of paralogous and accessory subunits, facilitating the study of these components in flies.

PRC1 and PRC2 coregulate a variety of cellular processes including embryonic development, differentiation, and cell proliferation (Chan and Morey 2019; Loubiere et al. 2019, Loubiere et al. 2020). Consistent with a role for PcG proteins in cell identity, dysregulation of these components has been associated with multiple types of cancer (Piunti and Shilatifard 2021), including breast and prostate cancers, as well as hematologic malignancies (Varambally et al. 2002; Guo et al. 2007; Li et al. 2010; Zhang et al. 2010; Ntziachristos et al. 2012; Herviou et al. 2016; Kim and Roberts 2016; Althobiti et al. 2020). In agreement, PRC1 loss-of-function mutations in *Drosophila* result in up-regulation of major oncogenes including JAK/STAT, NOTCH, and JNK signaling pathways, which are important drivers of the tumorigenic process (Classen et al. 2009; Martinez et al. 2009; Loubiere et al. 2016, Torres et al. 2018).

Recent studies also suggest a role for PRC1 in DNA double-strand break (DSB) repair by homologous recombination (HR) and, to a lesser extent, non-homologous end joining (NHEJ) (Vissers et al. 2012). Upon exposure to ionizing radiation (IR) or FokI-induced DSBs, PRC1 core subunits are quickly and transiently recruited to the damage site in an ATM-dependent manner, where they induce H2A/H2AXK119ub and transcriptional silencing (Kakarougkas et al. 2014, 2015; Ui et al. 2015). This histone modification also promotes the recruitment of DSB repair components including 53BP1, BRCA1, RAP80, and the resection protein CtIP (Ismail et al. 2010, Pan et al. 2011, Ismail et al. 2013, Kakarougkas et al. 2014, Fitieh et al. 2021, Fitieh et al. 2022). However, the extent to which DSB repair relies on PRC1 remains unclear, as loss of the PRC1 subunit BMI-1 only partially affects repair kinetics and the resulting sensitivity to IR exposure is modest (Ismail et al. 2010, Fitieh et al. 2021).

Importantly, even a transient depletion of PRC1 core complex subunits leads to cancer formation in *Drosophila* (Parreno et al. 2024). Specifically, a 24-h depletion of the PRC1 subunit PH results in irreversible activation of key members of the JAK–STAT pathway, which in turn trigger a switch to a self-sustaining cancer cell fate, even upon restoration of normal PRC1 activity (Parreno et al. 2024). These EICs are proficient in DSB repair and do not show chromosome rearrangements or major increase in the mutational load (Parreno et al. 2024).

Here, we investigate whether a sustained inactivation of PRC1, which mimics a cancer-inducing context, eventually results in DNA damage repair defects and genomic instability. We show that inactivation of PH over 5 days is sufficient to induce massive over-replication, the misregulation of several repair genes, and a broad reduction

in H2AK118ub and H3K27me3. Consistently, these tumors have elevated levels of endogenous DNA damage, DSB repair defects, and genomic instability. Together, these results are consistent with a model where EICs derived from transient PcG inactivation can rapidly transition to a state characterized by a highly genetically unstable genome. This instability might further contribute to tumor development when Polycomb depletion is maintained.

### **Materials and methods**

### Drosophila strains, genetics, and growth conditions

Drosophila flies were maintained on a standard corn-meal yeast extract medium at 25 °C. Crosses were performed as described in Parreno et al. (2024) (See also Fig. 1). Briefly, Gal80ts was used to achieve complete depletion of PH or the control white gene by switching the temperature from 18 °C to 29 °C. The ey-FLP system was used to generate complete knockdowns in the larval eye-antennal imaginal discs (EDs) (Parreno et al. 2024). Flies were reared and crossed at 18 °C to inhibit Gal4 activity. Six independent crosses were set up using 80 virgin females with 20 males for each genotype and egg laying was carried out for 4 h at 18 °C to synchronize the embryonic and larval development. As the timing of *Drosophila* development is temperaturedependent, we adapted the timing for each knockdown (KD) condition to carry out phenotypic and molecular analyses at comparable developmental times. Most dissections were performed on female larvae at the third instar larval stage (L3). Male larvae were used for the experiment described in Supplementary Fig. 2c,d. For achieving constant ph-KD and the temperature-matched white-KD control, tubes containing eggs were shifted to 29 °C throughout development, and third instar larvae (L3) were dissected 5 days after egg laying (AEL). The control no ph-KD was maintained at 18 °C throughout development (AEL to L3), with dissections typically done on day 11 AEL. For transient ph-KD at the L1 stage, flies were kept at 18 °C for 48 h, then shifted to 29 °C for 24 h and returned to 18 °C until dissection 11 days AEL (Parreno et al. 2024). For EdU experiments, transient ph-KD was induced at mid-L3 as follows: tubes were kept at 18 °C until 140 h AEL, shifted to 29 °C for 24 h and returned to 18 °C until dissection 24 h after the end of the temperature shift. Fly genotypes used for white-KD control were: ey-FLP, Act-gal4 (FRT.CD2 STOP) (BL#64,095), TubGal80ts (BL#7019), and UASwRNAi (BL#33,623)/UAS-GFP (BL#64,095). Fly genotypes used for ph-KD were: ey-FLP, Act-gal4 (FRT.CD2 STOP) (BL#64,095), TubGal80ts (BL#7019), and UAS-phRNAi (VDRC#50,028)/*UAS-GFP* (BL#64,095).



### Immunostaining and fluorescence microscopy

Third instar female larvae were dissected to isolate eyeantennal imaginal discs (EDs) at room temperature (RT) in 1×PBS. Tissues were fixed in 4% formaldehyde for 30 min on a rotating wheel. Permeabilization was carried out for 1 h in 1×PBS containing 0.5% Triton X-100 on a rotating wheel. Blocking was performed for 1 h using 3% BSA PBST  $(1 \times PBS + 0.1\% \text{ Triton } X-100)$ . Next, tissues were incubated with anti-yH2Av (1:500 prepared in 1% BSA PBST, Rockland, 600–401-914) for 2 h at RT. Samples were washed in 1×PBST for 15 min each for three times before adding a secondary antibody (donkey anti-rabbit Alexa Fluor 488, 1:1000 in 1% BSA PBST, Invitrogen, A-21206) for 2 h at RT, on a rotating wheel. Tissues were then washed in PBST for 15 min each for three times prior to DAPI staining at a final concentration of 1 µg/mL for 15 min. Discs were briefly washed in PBST and in  $1 \times PBS$ for 5 min each. Discs were mounted in Vectashield medium (Eurobio scientific, catalog no. H-1000-10) or ProLong Gold antifade agent (Life Technologies, P36930). Images for quantification of DSB foci were taken with a DeltaVision deconvolution microscope (GE Healthcare/Leica) using a 60× oil immersion objective (Olympus PlanApo N, NA 1.42) and a CoolSNAP HQ2 camera. Images were deconvolved using SoftWoRx 6.0.

### **EdU labeling to assess replication**

Ethynyl-2'-deoxyuridine (EdU, thymidine analog) labeling was performed using Click-iT Plus EdU Alexa fluor 555 Imaging kit (Invitrogen, #C10638) as per manufacturer's instructions. The EDs/tumors of female third instar larvae were dissected in Schneider's medium and EdU was added at a final concentration of 25 µM on a rotating wheel at RT for 15 min. After washing with PBS, tissues were fixed in 4% formaldehyde for 30 min and washed three times with PBS. The imaginal discs were permeabilized for 1 h in  $1 \times PBS + 0.5\%$  Triton X-100 on a rotating wheel then blocked for 1 h in  $1 \times PBS + 0.1\%$  Triton X-100 + 3% BSA. EdU detection was performed according to manufacturer's instructions for 30 min on a rotating wheel at RT away from light. 500 µl of Click-iT reaction solution was prepared per tube containing 10-12 EDs/tumor. After a wash with 1× PBS+0.1% Triton, DAPI staining was performed at a final concentration of 1 µg/ml for 15 min. Tissues were washes in  $1 \times PBS + 0.1\%$  Triton and discs were mounted in Vectashield medium. Image acquisition was performed using a Leica SP8-UV confocal microscope with a 10×objective (NA 0.4) and 63× oil immersion objective [numerical aperture (NA 1.4)]. Quantification of EdU-positive cells in Supplementary Fig. 2b was done over a single plane of cells using Fiji.

## Fluorescent In Situ Hybridization (FISH) for karyotype analysis

Chromosome preparation and FISH was performed as previously described (Gatti and Goldberg 1991; Larracuente and Ferree 2015; Ryu et al. 2015). Briefly, EDs or tumors from L3 larvae were dissected in 0.7% NaCl solution and incubated in colchicine solution (3 ml of 0.7% NaCl + 100 µl of 1 mM colchicine) for 1 h at RT away from light. Following colchicine treatment, tissues were incubated in 0.5% NaOAc for 7 min, and fixed using freshly prepared 2.5% PFA in 45% acetic acid for 4 min on a coverslip. Tissues were squashed onto poly-lysine coated slides and snap frozen in liquid nitrogen. The slides were washed in 100% ethanol for 5 min, air dried, and stained with FISH probes for AACAC, AATAT, and 359-bp repeats as previously described (Larracuente and Ferree 2015). Probe sequences are: 5'-6-FAM-(AACAC)7, 5'-Cy3-TTTTCCAAATTTCGGTCATCAAATAATCAT, and 5'-Cy5-(AATAT)6. Imaging was performed with a DeltaVision deconvolution microscope (GE Healthcare/Leica) using a 60× oil immersion objective (Olympus PlanApo, NA 1.42) and a CoolSNAP HQ2 camera. Images were processed deconvolved using SoftWoRx 6.0.

### Ionizing radiation exposure to induce DNA damage

Early L3 female larvae were transferred into a petri dish containing standard food medium and were irradiated with the dose of 5 Gy of X-rays using a Precision X-RAD iR160 irradiator. After irradiation, larvae were maintained in the petri dish at 29 °C. Larval heads were dissected at indicated timepoints at RT in 1×PBS and fixed in 4% paraformaldehyde for 30 min before immunostaining. Microscopy and image analysis were performed as described above. Due to accelerated pupation of L3 stage larvae at 29 °C, DSB repair analysis was limited to 4 h post-irradiation.

### **Bioinformatic analyses**

All in-house bioinformatic analyses were performed using R version 3.6.3 (URL: https://www.R-project.org/) and are publicly available at https://github.com/vloubiere/Rawal\_et\_al\_HCB\_2024.git. Computations on genomic coordinate files and downstream analyses were conducted using the data.table R package (data.table: Extension of 'data.frame'. https://r-datatable.com, https://Rdatatable.gitlab.io/data.table, https://github.com/Rdatatable/data.table, v1.14.2).

## Chromatin immunoprecipitation sequencing (ChIP-seq) and CUT&RUN data analysis

ChIP-seq datasets and the processed data files were downloaded from Gene Expression Omnibus (GEO) [GSE222193,



(Parreno et al. 2024)], and are listed Supplementary Table 1. PH ChIP-seq, and H2AK118Ub and H3K27me3 CUT&RUN coverage was computed using 2.5 kb bins covering all canonical chromosomes (X, ZL, ZR, ZL, ZR, ZL, ZR, ZL, ZR, ZL, ZR, ZL, ZR, ZL, ZL,

### RNA-seq data analysis

RNA-seq datasets and the processed output files were obtained from GEO (GSE222193, (Parreno et al. 2024)), and are listed in Supplementary Table 1. Differential expression analysis output, performed using the DESeq2 R package (Love et al. 2014) (v1.26.0), was obtained from Parreno et al. (2024).

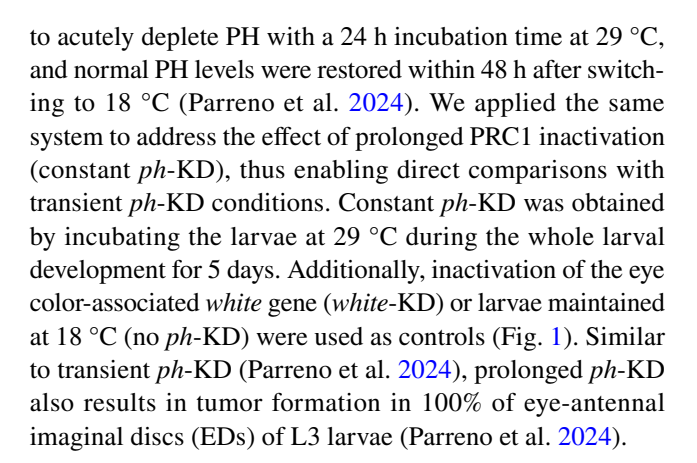
### **GO** terms enrichment

Gene Ontology (GO) terms associated to genes that were upregulated ( $p_{adi} < 0.05$  and  $log_2$  fold change > 1) or downregulated ( $p_{adi}$ < 0.05 and  $log_2$  fold change > 1) after constant or transient ph-KD were retrieved using the AnnnotationDbi R package (https://bioconductor.org/packages/Annotation Dbi.html, v1.48.0). For each GO term, over-representation was then assessed over a background set of genes consisting of all the genes that passed DESeq2 initial filters, using a one-sided Fisher's exact test (alternative = "greater"). Obtained p values were corrected for multiple testing using false discovery rate (FDR). Differentially expressed genes associated to "cellular response to DNA damage," "DNA repair," and "DNA replication" GO terms are available in Supplementary Table 2, together with six other genes which were associated to the "cellular response to DNA damage stimulus," which were nevertheless excluded from Fig. 3d due to the likelihood that their role in DNA damage response is indirect (Supplementary Table 2).

#### Results

# A fly system enables fine regulation of PH depletion during larval development

Recent studies showed that knocking down the PRC1 subunit PH for a short time (24 h, Fig. 1, transient *ph*-KD) during L1 larval stage is sufficient to induce EIC formation in third instar larvae (L3), and these EICs do not exhibit DNA repair defects or genomic instability (Parreno et al. 2024). These studies used an efficient thermosensitive *ph*-RNAi fly system



# Prolonged ph-KD results in H2AK118ub and H3K27me3 loss at Polycomb target sites

Given that both transient and constant ph-KD results in tumors characterized by loss of polarity and differentiation, we asked whether these tumors differ at the epigenetic level. We plotted the genome-wide enrichments of PH, H2AK118ub, and H3K27me3 from control EDs (no ph-KD), EICs after transient ph-KD, and tumors derived from constant ph-KD, using published ChIP-seq and CUT&RUN data sets [GSE222193 (Parreno et al. 2024), Supplementary Table 1]. Hilbert curves show that PH recruitment to chromatin is restored after transient ph-KD, whereas it is severely perturbed after constant ph-KD (Fig. 2a and Supplementary Fig. 1a). Consistently, the analysis of H2AK118ub and H3K27me3 enrichments around PRC1 target genes (PRC1bound) relative to PRC1 non-target genes (PRC1-unbound) shows that these modifications are largely restored after transient ph-KD, but not after constant ph-KD (Fig. 2b and Supplementary Fig. 1b). The most significant difference between EICs derived from transient ph-KD and constant ph-KD tumors is associated with H2AK118ub, consistent with this histone modification being the primary modification established by PRC1 (Fig. 2a,b and Supplementary Fig. 1b). We conclude that tumors resulting from prolonged ph-KD are characterized by extensive loss of H2AK118ub and H3K27me3 at PcG target genes, while this is not the case for EICs resulting from transient ph-KD.

## Prolonged *ph*-KD results in upregulation of DNA replication and repair genes

Given the major epigenetic differences between EICs generated by transient and constant *ph*-KD, we examined the differential gene expression between these tumors compared to control tissues (no *ph*-KD) and temperature-matched *white*-KD, using the published datasets derived from RNA-seq analyses (Parreno et al. 2024). As shown in Fig. 3a and Supplementary Fig. 1b, we found significant differences in gene



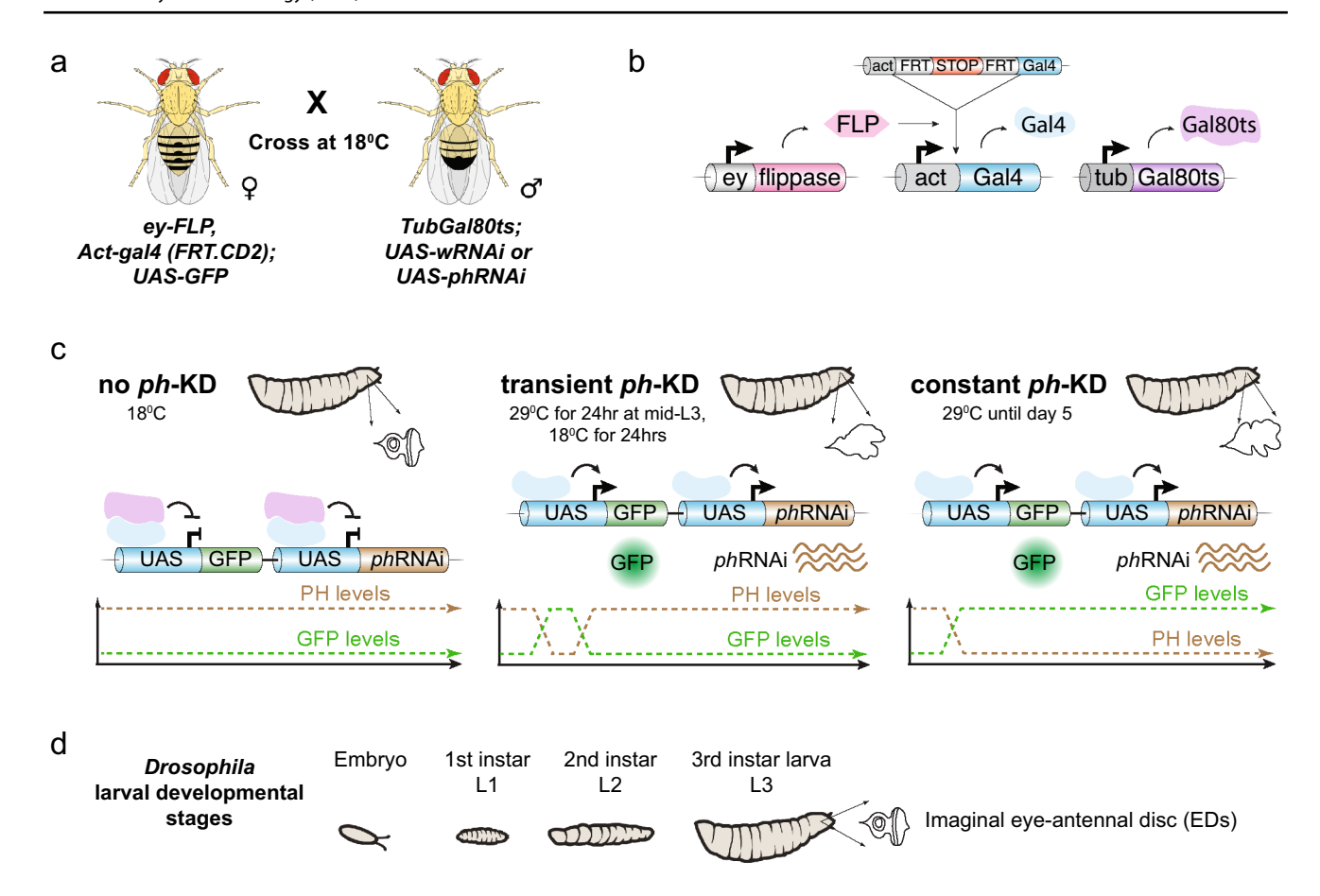


Fig. 1 Schematic representation of the experimental setup used to induce PRC1-dependent cancers. a Scheme of the experimental cross used to generate progeny with thermosensitive conditional knockdown using phRNAi or whiteRNAi. Female virgins from the fly line with ey-FLP, Act-gal4, and UAS-GFP were crossed with males from the fly line with tub-Gal80ts and UAS-phRNAi or UAS-wRNAi at 18 °C. b Expression of the flippase ey-FLP (pink) in imaginal eye-antennal disc (ED) cells catalyzes the FLP out of a transcriptional stop (red) in the developing discs, allowing the expression of act-Gal4 (light blue). Constitutively expressed tub-Gal80ts (pur-

ple) encodes a temperature-sensitive Gal4 repressor. **c** At 18 °C, TubGal80ts inhibits Gal4-mediated *phRNAi* as well as *GFP* expression (used as internal control), thereby maintaining high levels of PH, leading to normal ED development. **d** Shift of the developing embryo/larvae to the restrictive temperature of 29 °C for 24 h or 5 days leads to transient or constant *ph*-KD, respectively, thereby inducing tumors, which can be dissected at the third instar stage of larval development (L3). Image prepared in Adobe Illustrator and Photoshop. Fly schemes are from Wikimedia Commons

expression profiles between transient and constant *ph*-KD tumors. These include the upregulation of genes required for tissue and organ development in constant *ph*-KD tumors relative to transient *ph*-KD tumors, consistent with PRC1 roles in organismal development (Loubiere et al. 2019, Loubiere et al. 2020).

Remarkably, gene clusters corresponding to Gene Ontology (GO) terms related to DNA replication, DNA damage, and DNA repair were also mostly upregulated in constant ph-KD conditions relative to transient ph-KD tumors (Fig. 3a). Consistently, a fold-change analysis of all the genes classified as "DNA replication" (n = 111) or "DNA damage response" (n = 242) shows a significantly higher level of transcription for both categories in constant ph-KD tumors relative to control, and also compared to all genes

(Supplementary Fig. 1c). This indicates that DNA replication and DNA damage response genes are overall more transcriptionally active in tumors derived from sustained *ph*-KD.

Within this general trend, 21 genes required for "DNA replication" and 28 genes required for the "DNA damage response" were the most affected, displaying at least a twofold change in expression in constant *ph*-KD tumors relative to controls, most of which (18 and 26 genes, respectively) were upregulated (Fig. 3b, c).

Most of the DNA replication and DNA damage response genes upregulated in tumors derived from constant *ph*-KD are not associated with PRC1 enrichments in normal tissues (no *ph*-KD) (e.g., Fig. 3d, CG10336 or TIPIN in mammals), suggesting that they are not direct targets of PH and their upregulation is an indirect effect of PRC1 loss.



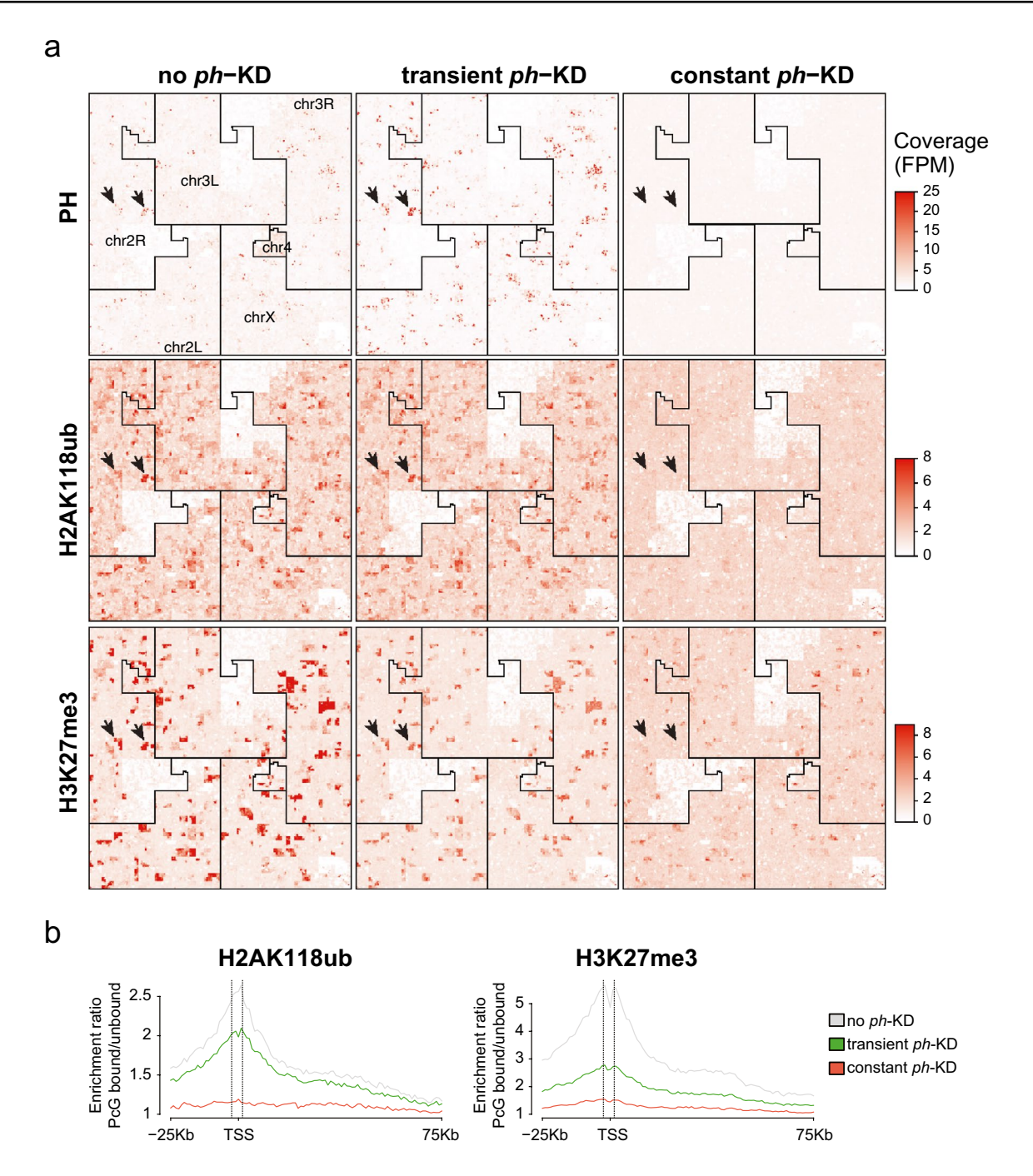


**Fig. 2 Tumors induced by constant** *ph***-KD display loss of H2AK118ub and H3K27me3 at PcG target genes. a** Hilbert curves display the enrichment of PH, H2AK118ub and H3K27me3 in control (no *ph*-KD), transient *ph*-KD, and constant *ph*-KD conditions, along all the chromosomes (see also Supplementary Fig. 1a). Black arrows indicate examples of enrichments of PH, H2AK118ub, and H3K27me3 at representative PRC1-target sites. Each chromosome/

arm is outlined with a black line. Scales on the right indicate enrichment levels. FPM: fragments per million reads. **b** Enrichment ratios of H2AK118ub (left) and H3K27me3 (right) marks around the TSS (-25 to + 75 Kb) of PcG-bound genes compared relative to a control set of activity-matched, PcG-unbound genes (n = 610 genes for each group) in tissues from indicated KD conditions

The most notable exception is the gene for the replication, repair, and transcription factor Fkh (FOXA2 and FOXA1 in mammals) (Knott et al. 2012, Li et al. 2012, Dummer et al. 2016, Jin et al. 2020, Hoggard et al. 2021), whose promoter

is enriched for PRC1 in normal tissues. This suggests that PRC1 downregulation from constant *ph*-KD directly affects *fkh* expression (Fig. 3d).



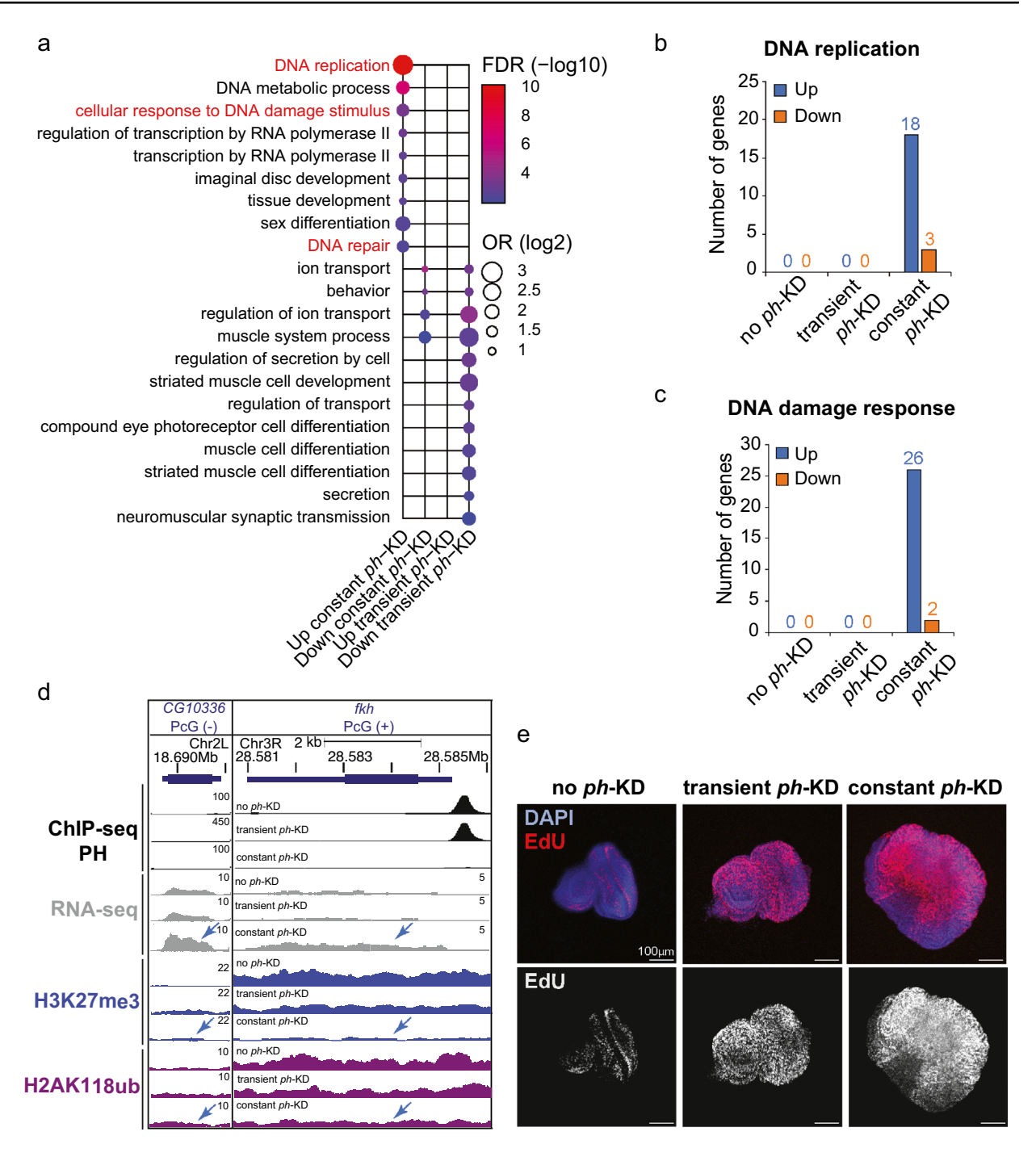


Fig. 3 Tumors induced by constant *ph*-KD display dysregulation of DNA damage response- and replication -associated genes. a Representative GO terms enriched in genes differentially expressed after constant *ph*-KD or transient *ph*-KD (up- or down- regulation). The complete list is shown in Supplementary Fig. 1c. b Number of genes specifically dysregulated after constant *ph*-KD associated with "DNA replication" GO term. c Number of genes specifically dysregulated after constant *ph*-KD and associated with "DNA damage

response" GO term. **d** Genome browser snapshots for representative genes upregulated only in constant ph-KD conditions showing PH, H2AK118ub, and H3K27me3 normalized tracks (ChIP-seq or CUT&RUN, normalized by input) and gene expression by RNA-seq, in control (no ph-KD), transient ph-KD, and constant ph-KD conditions. **e** EdU staining of EDs and tumors from L3 in indicated KD conditions

The replication genes affected in constant *ph*-KD tumors correspond to key replication components, including the

MCM complex, origin firing factors, and several DNA polymerases (Supplementary Table 2). This increase in



**Table 1 List of DNA repair genes dysregulated genes upon constant** *ph***-KD. Selected genes from Supplementary Table 2, including their DNA repair function, mammalian homologs, and link to cancer. Mismatch repair (MMR), base excision repair (BER), nucleotide excision repair (NER), translesion synthesis (TLS)** 

Drosophila gene	Mammalian homolog	Function in DNA repair	Link to cancer
Upregulated			
Mms4	EME1	Holliday Junction resolvase in complex with Mus81. Replication fork processing and repair	Overexpressed in several cancers, including colorectal and lung cancer. Associated with poor prognosis and chemo resistance
RecQ4	RECQ4	HR repair	Overexpressed in several cancers, including osteosarco- mas, prostate, colorectal, and breast cancers. Associ- ated with poor prognosis and chemo resistance
PolH	POLH	Translesion polymerase	Overexpressed in several cancers, including breast, lung, ovarian and bladder cancers. Associated with poor prognosis and chemoresistance
CG43295	MRNIP	HR repair through phase separation, fork protection	Overexpressed in colorectal cancer, associated with radioresistance and poor prognosis
FANCI	FANCI	Interstrand crosslink repair, stalled fork processing	Overexpressed in several cancers, including lung adeno- carcinoma, cervical cancer and liver hepatocellular carcinoma, associated with poor cancer prognosis
Spel1 Mlh1 Msh6	MSH2 MLH1 MSH6	Mismatch repair, Homeologous recombination	Commonly overexpressed in cancer, correlated with poor prognosis in prostate cancer
Rif1	RIF1	Telomere maintenance, DSB repair (prevents resection, promoting NHEJ)	Commonly overexpressed in cancer, promotes drug resistance, correlated with poor prognosis
CG10336	TIPIN	Fork protection complex,	Overexpression induces cancer, promotes drug resist-
Timeout/tim2	TIMELESS	Replication stress response, Homologous recombination repair, Telomere maintenance	ance, associated with poor cancer prognosis
Claspin	CLASPIN	Checkpoint activation in response to replication stress	Overexpression induces cancer, promotes radioresistance, associated with poor prognosis
Downregulated			
PCNA2	PCNA	Sliding clamp for DNA repair in <i>Drosophila</i> . HR, MMR, NER, BER, TLS,	Downregulated in many cancers, particularly in sarcomas and testicular cancer

expression of replication-linked genes might result from an overall induction of replication in the tissue. Thus, we investigated the proliferation state of the cells in these tumors by EdU staining. As expected, control EDs are characterized by a few replicating cells posteriorly to the morphogenetic furrow (Avellino et al. 2023; Parreno et al. 2024) (Fig. 3a and Supplementary Fig. 2a,b). Conversely, tumors derived from constant ph-KD are characterized by massive EdU incorporation, indicating the switch to an uncontrolled overproliferating state (Fig. 3a and Supplementary Fig. 2a,b). Of note, DNA replication-associated genes are found overexpressed also in transient ph-KD tumors (Supplementary Fig. 1d), albeit to a lesser extent compared to constant ph-KD tumors. Consistently, transient ph-KD tumors are also enriched for replicating cells compared to controls (Parreno et al. 2024) (Fig. 3e and Supplementary Fig. 2a,b), although the number of replicating cells in these tumors is lower compared with tumors derived from constant *ph*-KD (Supplementary Fig. 2a,b).

Together, these results establish that constant ph-KD leads to tumors characterized by the upregulation of several DNA replication genes, which is likely a consequence of cell hyperproliferation. This upregulation is more pronounced than that observed in tumors derived from transient ph-KD, consistent with an higher proliferation rate. Upregulation of components required for replication initiation and progression can also contribute to the acquisition of the hyperproliferative state (Yu et al. 2020). In addition, we observed dysregulation of several DNA damage response genes upon constant depletion of PH, most of which are likely the indirect consequence of PH loss. These genes are mostly expressed at normal levels in transient ph-KD tumors, representing a major difference between the effects of short-term and long-term PH depletions.



### Prolonged *ph*-KD leads to defective DSB repair and increased genomic instability

DNA repair genes over-expressed in constant ph-KD tumors include several components previously linked to damage accumulation, cancer formation, and/or poor cancer prognosis (Table 1), like Mms4 (Dewalt et al. 2014), RecQ4 (Maire et al. 2009; Su et al. 2010; Xu et al. 2021), PolH (Tomicic et al. 2014, Sonobe et al. 2024), Tipin/Timeless (Zhou et al. 2020; Chen et al. 2022), Claspin (Choi et al. 2014), MRNIP (Staples et al. 2016, Bennett et al. 2020, Wang et al. 2022), FANCI (Smogorzewska et al. 2007; Li et al. 2023), MMR proteins (Msh2, Mlh1, Msh6) (Shcherbakova and Kunkel 1999; Velasco et al. 2002; Li et al. 2008; Wagner et al. 2016; Wilczak et al. 2017; Chakraborty et al. 2018; Donis et al. 2021; Zhou et al. 2024), and Rif1 (Liu et al. 2018; Mei et al. 2018; Sad et al. 2021). Similarly, genes downregulated in constant ph-KD tumors include known components required for DNA repair and replication fork protection in the presence of replication damage, such as the PCNA variant PCNA2 (Feng et al. 2023) (Table 1). Collectively, misregulation of these genes is expected to lower fork protection, increase DSB formation in response to stalled fork, and impair DSB repair.

We directly tested this by investigating DNA break formation through immunofluorescence (IF) analysis of γH2Av foci in tumors dissected from L3 larvae after constant *ph*-KD or in EDs from the temperature-matched *wRNAi* control. Constant *ph*-KD results in a threefold increase in the number of γH2Av foci in the tissue, indicating a higher level of endogenous DNA damage (Fig. 4a–c). This likely derives from the higher number of replicating cells, which typically experience a higher baseline level of damage than non-replicating cells, along with defective fork protection and repair.

In addition, we investigated the DSB repair response by treating constant ph-KD tumors and their controls with 5 Gy ionizing radiation (IR), and by quantifying the kinetics of yH2Av focus formation and resolution (Fig. 4c). Both tumor and ED control tissues showed a significant increase in the number of yH2Av foci 30 min after IR, indicating DSB induction and checkpoint activation. The higher level of repair foci in ph-KD tumors relative to the control reflects the higher baseline level of damage (Fig. 4c, timepoint 0). Importantly, constant ph-KD tumors display a significantly higher number of yH2Av foci relative to control EDs 4 h after irradiation, and this difference is much more pronounced than what is observed in untreated (UNT, timepoints 0) tissues or in tissues fixed 30 min after IR (Fig. 4b,c). This indicates that, unlike transient ph-KD tumors (Parreno et al. 2024), constant ph-KD tumors are defective in DSB repair.

Given the higher amount of DNA damage and defective repair, we hypothesized that constant ph-KD tumors might accumulate unrepaired DSBs over time, resulting in chromosome rearrangements and genomic instability. We tested this by karyotype analysis of tumors from constant ph-KD and EDs from wRNAi control in L3 larvae (Fig. 4d). We stained with FISH probes for pericentromeric regions of different chromosomes to facilitate chromosome detection in rearranged conditions. Remarkably, we observe a six-fold increase in the frequencies of chromosome rearrangements in constant ph-KD tumors relative to controls (Fig. 4d,e). Rearrangements include a large number of chromosome fusions, aneuploidies, and abnormal number of satellites (Fig. 4d,e). Moreover, we observe a significant increase in a rare form of rearrangements characterized by fusions across several chromosomes ("broad rearrangements") (Fig. 4d, e). The increase in chromosome rearrangements occurred in both males and females, suggesting that the effect is not sex-specific (Supplementary Fig. 2c,d).

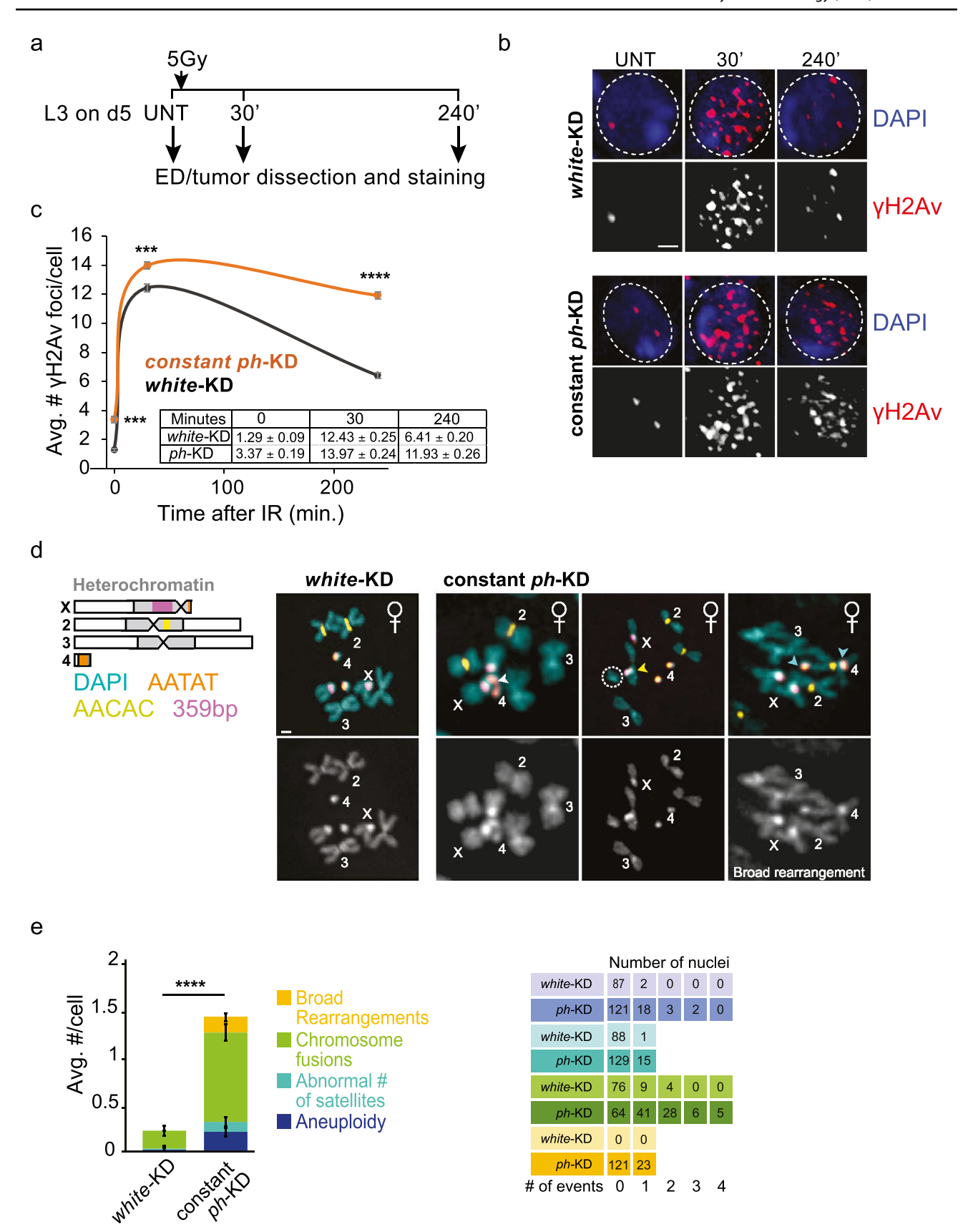
In conclusion, tumors induced by PH depletion over 5 days during larval stages are characterized by misregulation of genes required for replication fork protection and DNA repair, DSB repair defects, and widespread genome instability, which was not observed in EICs derived from transient *ph*-KD.

### **Discussion**

Chromosomal instability is a common hallmark of both human (Hanahan and Weinberg 2011) and fly tumors (Gateff and Schneiderman 1974; Basto et al. 2008; Torres et al. 2010; Dekanty et al. 2012), and it can contribute to tumor invasiveness (Barrio et al. 2023). However, the cause-effect relationship between abnormal karyotypes and tumor progression remains debatable [reviewed in (Fukasawa 2005; Milan et al. 2014)] and consistently, how tumors associated with PRC1 dysregulation acquire genome instability was unclear. Our comparative analysis of epigenetically initiated cancers due to transient ph-KD and tumors resulting from prolonged ph-KD offers a rare opportunity to identify progressive changes occurring in a developing tumor. These studies shed light on how epigenetic tumors with a stable genome can quickly transition into a state characterized by massive genomic instability through prolonged PRC1 inactivation (Fig. 5).

We show that, unlike transient *ph*-KD (Parreno et al. 2024), constant *ph*-KD results in loss of H2AK118ub and H3K27me3 at Polycomb target genes, dysregulation of several DNA repair genes, marked defects in DSB repair, and widespread genome instability. Importantly, the transition to a tumor characterized by an unstable genome is reached







√Fig. 4 Constant ph-KD tumors are characterized by DSB repair defects and genomic instability. a Schematic representation of the experiment used to assess DSB repair. b Representative images of Drosophila cells from EDs or tumors, stained for yH2Av before (UNT) and at the indicated timepoints after IR, from white-KD (control) and constant ph-KD conditions. Dashed circles indicate the position of each nucleus, identified by DAPI staining. c Quantification of the number of γH2Av foci per cell before (0 min) and after irradiation (30 and 240 min) in EDs or tumors derived from white-KD (control) and constant ph-KD.  $n \ge 100$  cells per replicate, representing EDs or tumors from three distinct larvae and independent crosses, at the indicated time points from IR exposure. Error bars, standard error of the mean (SEM). Statistical significance was calculated using a two-sided t-test: \*\*\*\*p value < 1  $\times$  10<sup>-5</sup>. The table show the individual average values and corresponding SEM. d Examples of karyotypes from white-KD (control) and constant ph-KD EDs or tumors from female larvae, showing examples of different chromosomal abnormalities. The scheme of the chromosomes shows the position of the major satellites stained by FISH. White arrowheads: fusions between Chr 4 and Chr X, and between two Chr 4. Dashed circle: chromosome fragment derived from a fusion between Chr 3 and X (yellow arrowhead). Cyan arrowheads: fusions between Chr 4 and Chr 2, in addition to broad rearrangements. e Quantification of chromosome abnormalities in EDs or tumors from white-KD (control) and constant ph-KD flies. For each type of abnormality (see color legend), the number of counted events are shown on the right. n=89 karyotypes representing EDs from three larvae from independent crosses for white-KD. n = 144 karyotypes representing tumors from seven larvae from independent crosses for ph-KD. Error bars, SEM. \*\*\*\*p value  $< 1 \times 10^{-5}$ . Statistical significance was calculated using a two-sided t-test. Scale bars,1 µm

within only 5 days of PH depletion, revealing a rapid acquisition of this typical cancerous phenotype.

However, transient *ph*-KD tumors already display a hyperproliferating state and some level of misregulation of replication genes. This suggests a progression of the tumor where the hyperproliferating state is acquired first, resulting in a higher baseline level of damage, followed by dysregulation of fork protection and repair genes (including PRC1 itself), which in turn results in DNA repair defects and chromosome rearrangements. Loss of PRC1 function

can contribute to these phenotypes in non-mutually exclusive ways: (i) by increasing transcription globally, thus bolstering replication stress form replication-transcription collision (Zeman and Cimprich 2014, Hamperl et al. 2017, Gomez-Gonzalez and Aguilera 2019, Chakraborty et al. 2023); (ii) by preventing the establishment of H2AK118ub and H3K27me3 at DSBs, thus interfering with DSB repair (Ismail et al. 2010, Campbell et al. 2013, Ismail et al. 2013, Fitieh et al. 2021, Fitieh et al. 2022); and (iii) by misregulating the expression of genes required for replication, DNA fork protection and DSB repair, thus increasing the accumulation of unrepaired and misrepaired breaks. In addition, these defects are amplified in a context of a hyperproliferating tissue, with additional potential for replication damage. Collectively, tumors derived from transient or constant ph-KD represent a promising model system to investigate the gradual epigenetic and genomic changes leading to cancer formation.

Together, these observations also highlight the importance of core PRC1 subunits as tumor suppressors and guardians of genome stability. The finding that transient PRC1 depletion leads to epigenetic tumors without inducing genome instability, while prolonged inactivation of this complex results in DNA repair defects and massive genome rearrangements, is also important to inform cancer treatment approaches. PRC1 has been considered a potential therapeutic target for cancer (Shukla et al. 2021; Itoh et al. 2022; Park et al. 2023) and our study suggests that PRC1 inactivation will likely increase the sensitivity of tumor cells to DNA damaging agents. On the other hand, "epi-drugs" targeting PRC1 can also potentially transform healthy tissues into epigenetically initiated cancers and induce genome instability in response to protracted treatments. Thus, understanding how epigenetic tumors acquire a state characterized by high genome instability is important for establishing improved and safer approaches for cancer therapy.

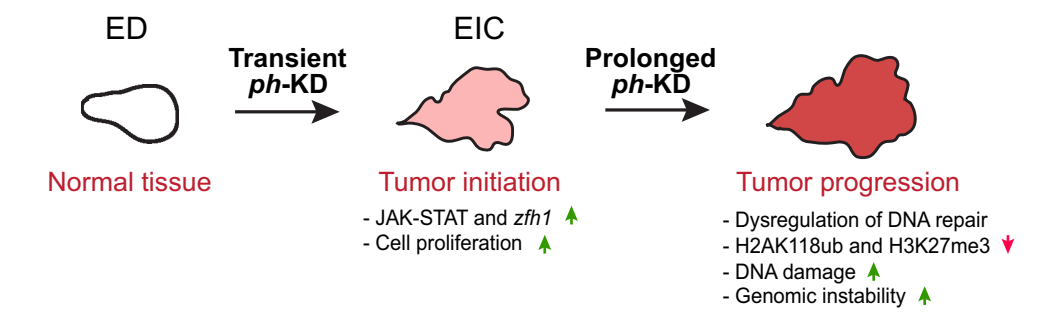


**Fig. 5 Model for tumor progression in EICs.** Upon transient ph-KD, EDs switch to a hyperproliferative cell fate notably due to an irreversible activation of the JAK–STAT pathway and *zfh1* (Parreno et al. 2024). Prolonging *ph*-KD for 4 additional days results in accumulation of replication damage, misregulation of DNA dam-

age response genes, defective DSB repair leading to persistent DNA damage. This progression reflects a cascade of events where initial hyperproliferation leads to increased replication stress and subsequent dysregulation of DNA repair mechanisms, culminating in genome instability



**Supplementary Information** The online version contains supplementary material available at https://doi.org/10.1007/s00418-024-02302-z.

Acknowledgements We wish to thank Bernd Schuettengruber for the training of Juliette Gracia and help with the generation of tumor tissues and genomics data. We thank all the members of the Chiolo and Cavalli Labs for helpful discussions. We also thank John Tower and Derrick Morton for access to their fly incubators.

Author contributions C.C.R. carried out the conceptualization, writing (original draft preparation, reviewing, and editing,) investigation, and figure preparation. V.L. performed the data analysis and writing (reviewing and editing). V.P performed the investigation and writing (reviewing and editing). N.L.B. performed the investigation, figure preparation, and writing (reviewing and editing). J.G. performed the investigation, figure preparation, and writing (reviewing and editing). C.M. performed the investigation, figure preparation, and writing (reviewing and editing). A.-M.M., C.G, and I.C. carried out the conceptualization, supervision, funding acquisition, and writing (reviewing and editing).

Funding Open access funding provided by SCELC, Statewide California Electronic Library Consortium. This work was supported by R01GM117376 and National Science Foundation Career Grant 1751197 to I.C. The laboratory of G.C. was supported by grants from the European Research Council (Advanced Grant 3DEpi, under grant agreement number 788972), the European Union (CHROM-DESIGN Project, under the Marie Skłodowska- Curie grant agreement number 813327), the Fondation pour la Recherche Médicale (EQU202303016280), the MSDAVENIR foundation (project GENE-IGH), the INSERM, the Centre National pour la Recherche Scientifique, the Agence Nationale de la Recherche (E- RARE project 'IMPACT' and "PLASMADIFF3D" project, ANR-18-CE15-0010), by the Fondation ARC (contract no. 216574, acronym 'Epicancer') and by the French National Cancer Institute (INCa PLBIO18-362).

**Data availability** Data from this study will be available from the corresponding authors upon reasonable request.

**Code availability** All custom scripts were made publicly available at https://github.com/vloubiere/Rawal\_et\_al\_HCB\_2024.git

#### **Declarations**

**Conflict of interest** The authors have no relevant financial or non-financial interests to disclose.

Informed consent Not applicable.

**Human and animal rights** The study did not involve any human or animal subjects.

Open Access This article is licensed under a Creative Commons Attribution 4.0 International License, which permits use, sharing, adaptation, distribution and reproduction in any medium or format, as long as you give appropriate credit to the original author(s) and the source, provide a link to the Creative Commons licence, and indicate if changes were made. The images or other third party material in this article are included in the article's Creative Commons licence, unless indicated otherwise in a credit line to the material. If material is not included in the article's Creative Commons licence and your intended use is not permitted by statutory regulation or exceeds the permitted use, you will need to obtain permission directly from the copyright holder. To view a copy of this licence, visit http://creativecommons.org/licenses/by/4.0/.



- Althobiti M, Muftah AA, Aleskandarany MA, Joseph C, Toss MS, Green A, Rakha E (2020) The prognostic significance of BMI1 expression in invasive breast cancer is dependent on its molecular subtypes. Breast Cancer Res Treat 182(3):581–589
- Anders S (2009) Visualization of genomic data with the Hilbert curve. Bioinformatics 25(10):1231–1235
- Avellino A, Peng CH, Lin MD (2023) Cell cycle regulation by NF-YC in drosophila eye imaginal disc: implications for synchronization in the non-proliferative region. Int J Mol Sci 24(15):12203
- Barbour H, Daou S, Hendzel M, Affar EB (2020) Polycomb groupmediated histone H2A monoubiquitination in epigenome regulation and nuclear processes. Nat Commun 11(1):5947
- Barrio L, Gaspar AE, Muzzopappa M, Ghosh K, Romao D, Clemente-Ruiz M, Milán M (2023) Chromosomal instability-induced cell invasion through caspase-driven DNA damage PMID: 37751744 Curr Biol Oct 23;33(20):4446–4457. PMID: 37751744e5. https:// doi.org/10.1016/j.cub.2023.09.004
- Basto R, Brunk K, Vinadogrova T, Peel N, Franz A, Khodjakov A, Raff JW (2008) Centrosome amplification can initiate tumorigenesis in flies. Cell 133(6):1032–1042
- Bennett LG, Wilkie AM, Antonopoulou E, Ceppi I, Sanchez A, Vernon EG, Gamble A, Myers KN, Collis SJ, Cejka P, Staples CJ (2020) MRNIP is a replication fork protection factor. Sci Adv 6(28):eaba974
- Blackledge NP, Farcas AM, Kondo T, King HW, McGouran JF, Hanssen LLP, Ito S, Cooper S, Kondo K, Koseki Y, Ishikura T, Long HK, Sheahan TW, Brockdorff N, Kessler BM, Koseki H, Klose RJ (2014) Variant PRC1 complex-dependent H2A ubiquitylation drives PRC2 recruitment and polycomb domain formation. Cell 157(6):1445–1459
- Campbell S, Ismail IH, Young LC, Poirier GG, Hendzel MJ (2013) Polycomb repressive complex 2 contributes to DNA double-strand break repair. Cell Cycle 12(16):2675–2683
- Chakraborty U, Dinh TA, Alani E (2018) Genomic instability promoted by overexpression of mismatch repair factors in yeast: a model for understanding cancer progression. Genetics 209(2):439–456
- Chakraborty S, Schirmeisen K, Lambert SA (2023) The multifaceted functions of homologous recombination in dealing with replication-associated DNA damages. DNA Repair (amst) 129:103548
- Chan HL, Morey L (2019) Emerging roles for Polycomb-group proteins in stem cells and cancer. Trends Biochem Sci 44(8):688-700
- Chen H, Zhang C, Zhou Q, Guo Y, Ren Z, Yu Z (2022) Integrated bioinformatic analysis identifies TIPIN as a prognostic biomarker in hepatocellular carcinoma. Dis Markers 2022:5764592
- Choi SH, Yang H, Lee SH, Ki JH, Nam DH, Yoo HY (2014) TopBP1 and Claspin contribute to the radioresistance of lung cancer brain metastases. Mol Cancer 13:211
- Classen AK, Bunker BD, Harvey KF, Vaccari T, Bilder D (2009) A tumor suppressor activity of Drosophila Polycomb genes mediated by JAK-STAT signaling. Nat Genet 41(10):1150–1155
- Cooper S, Grijzenhout A, Underwood E, Ancelin K, Zhang T, Nesterova TB, Anil-Kirmizitas B, Bassett A, Kooistra SM, Agger K, Helin K, Heard E, Brockdorff N (2016) Jarid2 binds mono-ubiquitylated H2A lysine 119 to mediate crosstalk between Polycomb complexes PRC1 and PRC2. Nat Commun 7:13661
- Dekanty A, Barrio L, Muzzopappa M, Auer H, Milan M (2012) Aneuploidy-induced delaminating cells drive tumorigenesis in Drosophila epithelia. Proc Natl Acad Sci U S A 109(50):20549–20554
- Dewalt RI, Kesler KA, Hammoud ZT, Baldridge L, Hattab EM, Jalal SI (2014) Gastroesophageal junction adenocarcinoma displays abnormalities in homologous recombination and nucleotide excision repair. Lung Cancer (auckl) 5:11–20



- Donis SP, Gonzalez AP, Alves MGO, do Carmo Carvalho BF, Ferreira CCP, Almeida JD, Iruegas EP, Petronacci CMC, Penaranda JMS, Sayans MP (2021) MLH1, MSH2, MRE11, and XRCC1 in Oral Leukoplakia and oral squamous cell carcinoma. Appl Immunohistochem Mol Morphol 29(8):613–618
- Dummer AM, Su Z, Cherney R, Choi K, Denu J, Zhao X, Fox CA (2016) Binding of the Fkh1 Forkhead associated domain to a phosphopeptide within the Mph1 DNA helicase regulates mating-type switching in budding yeast. PLoS Genet 12(6):e1006094
- Feng Y, Xia S, Hui J, Xu Y (2023) Circular RNA circBNC2 facilitates glycolysis and stemness of hepatocellular carcinoma through the miR-217/high mobility group AT-hook 2 (HMGA2) axis. Heliyon 9(6):e17120
- Fitieh A, Locke AJ, Mashayekhi F, Khaliqdina F, Sharma AK, Ismail IH (2022) BMI-1 regulates DNA end resection and homologous recombination repair. Cell Rep 38(12):110536
- Fitieh A, Locke AJ, Motamedi M, Ismail IH (2021) The role of Polycomb group protein BMI1 in DNA repair and genomic stability. Int J Mol Sci 22(6):2976
- Fukasawa K (2005) Centrosome amplification, chromosome instability and cancer development. Cancer Lett 230(1):6–19
- Gateff E, Schneiderman HA (1974) Developmental capacities of benign and malignant neoplasms of Drosophila. Wilhelm Roux Arch Entwickl Mech Org 176(1):23–65
- Gatti M, Goldberg ML (1991) Mutations affecting cell division in Drosophila. Methods Cell Biol 35:543–586
- Gomez-Gonzalez B, Aguilera A (2019) Transcription-mediated replication hindrance: a major driver of genome instability. Genes Dev 33(15–16):1008–1026
- Guo WJ, Zeng MS, Yadav A, Song LB, Guo BH, Band V, Dimri GP (2007) Mel-18 acts as a tumor suppressor by repressing Bmi-1 expression and down-regulating Akt activity in breast cancer cells. Cancer Res 67(11):5083–5089
- Hamperl S, Bocek MJ, Saldivar JC, Swigut T, Cimprich KA (2017) Transcription-replication conflict orientation modulates r-loop levels and activates distinct DNA damage responses. Cell 170(4):774–786
- Hanahan D, Weinberg RA (2011) Hallmarks of cancer: the next generation. Cell 144(5):646–674
- Herviou L, Cavalli G, Cartron G, Klein B, Moreaux J (2016) EZH2 in normal hematopoiesis and hematological malignancies. Oncotarget 7(3):2284–2296
- Hoggard T, Hollatz AJ, Cherney RE, Seman MR, Fox CA (2021) The Fkh1 Forkhead associated domain promotes ORC binding to a subset of DNA replication origins in budding yeast. Nucleic Acids Res 49(18):10207–10220
- Holoch D, Margueron R (2017) Mechanisms regulating PRC2 recruitment and enzymatic activity. Trends Biochem Sci 42(7):531–542
- Hopkins JL, Lan L, Zou L (2022) DNA repair defects in cancer and therapeutic opportunities. Genes Dev 36(5–6):278–293
- Ismail IH, Andrin C, McDonald D, Hendzel MJ (2010) BMI1-mediated histone ubiquitylation promotes DNA double-strand break repair. J Cell Biol 191(1):45–60
- Ismail IH, McDonald D, Strickfaden H, Xu Z, Hendzel MJ (2013) A small molecule inhibitor of polycomb repressive complex 1 inhibits ubiquitin signaling at DNA double-strand breaks. J Biol Chem 288(37):26944–26954
- Itoh Y, Takada Y, Yamashita Y, Suzuki T (2022) Recent progress on small molecules targeting epigenetic complexes. Curr Opin Chem Biol 67:102130
- Jin Y, Liang Z, Lou H (2020) The emerging roles of fox family transcription factors in chromosome replication, organization, and genome stability. Cells 9(1):258
- Kakarougkas A, Ismail A, Chambers AL, Riballo E, Herbert AD, Kunzel J, Lobrich M, Jeggo PA, Downs JA (2014) Requirement for PBAF

- in transcriptional repression and repair at DNA breaks in actively transcribed regions of chromatin. Mol Cell 55(5):723-732
- Kakarougkas A, Downs JA, Jeggo PA (2015) The PBAF chromatin remodeling complex represses transcription and promotes rapid repair at DNA double-strand breaks. Mol Cell Oncol 2(1):e970072
- Kasinath V, Beck C, Sauer P, Poepsel S, Kosmatka J, Faini M, Toso D, Aebersold R, Nogales E (2021) JARID2 and AEBP2 regulate PRC2 in the presence of H2AK119ub1 and other histone modifications. Science. https://doi.org/10.1126/science.abc3393
- Kassis JA, Kennison JA, Tamkun JW (2017) Polycomb and trithorax group genes in Drosophila. Genetics 206(4):1699–1725
- Kim KH, Roberts CW (2016) Targeting EZH2 in cancer. Nat Med 22(2):128–134
- Knott SR, Peace JM, Ostrow AZ, Gan Y, Rex AE, Viggiani CJ, Tavare S, Aparicio OM (2012) Forkhead transcription factors establish origin timing and long-range clustering in S. cerevisiae. Cell 148(1–2):99–111
- Larracuente AM, Ferree PM (2015) Simple method for fluorescence DNA in situ hybridization to squashed chromosomes. J vis Exp 95:52288
- Levine SS, Weiss A, Erdjument-Bromage H, Shao Z, Tempst P, Kingston RE (2002) The core of the polycomb repressive complex is compositionally and functionally conserved in flies and humans. Mol Cell Biol 22(17):6070–6078
- Li M, Liu L, Wang Z, Wang L, Liu Z, Xu G, Lu S (2008) Overexpression of hMSH2 and hMLH1 protein in certain gastric cancers and their surrounding mucosae. Oncol Rep 19(2):401–406
- Li W, Li Y, Tan Y, Ma K, Cui J (2010) Bmi-1 is critical for the proliferation and invasiveness of gastric carcinoma cells. J Gastroenterol Hepatol 25(3):568–575
- Li J, Coic E, Lee K, Lee CS, Kim JA, Wu Q, Haber JE (2012) Regulation of budding yeast mating-type switching donor preference by the FHA domain of Fkh1. PLoS Genet 8(4):e1002630
- Li W, Yu M, Zhang J, Huang J, Lin Z, Chen J, Jiang G, Lin X (2023) High expression levels of FANCI correlate with worse prognosis and promote tumor growth of lung adenocarcinoma partly via suppression of M1 macrophages. Gene 851:147053
- Liu YB, Mei Y, Long J, Zhang Y, Hu DL, Zhou HH (2018) RIF1 promotes human epithelial ovarian cancer growth and progression via activating human telomerase reverse transcriptase expression. J Exp Clin Cancer Res 37(1):182
- Loubiere V, Delest A, Thomas A, Bonev B, Schuettengruber B, Sati S, Martinez AM, Cavalli G (2016) Coordinate redeployment of PRC1 proteins suppresses tumor formation during Drosophila development. Nat Genet 48(11):1436–1442
- Loubiere V, Martinez AM, Cavalli G (2019) Cell fate and developmental regulation dynamics by polycomb proteins and 3D genome architecture. BioEssays 41(3):e1800222
- Loubiere V, Papadopoulos GL, Szabo Q, Martinez AM, Cavalli G (2020) Widespread activation of developmental gene expression characterized by PRC1-dependent chromatin looping. Sci Adv 6(2):eaax001
- Love MI, Huber W, Anders S (2014) Moderated estimation of fold change and dispersion for RNA-seq data with DESeq2. Genome Biol 15(12):550
- Maire G, Yoshimoto M, Chilton-MacNeill S, Thorner PS, Zielenska M, Squire JA (2009) Recurrent RECQL4 imbalance and increased gene expression levels are associated with structural chromosomal instability in sporadic osteosarcoma. Neoplasia 11(3):260–268 (263p following 268)
- Martinez AM, Schuettengruber B, Sakr S, Janic A, Gonzalez C, Cavalli G (2009) Polyhomeotic has a tumor suppressor activity mediated by repression of Notch signaling. Nat Genet 41(10):1076–1082



- Mei Y, Liu YB, Cao S, Tian ZW, Zhou HH (2018) RIF1 promotes tumor growth and cancer stem cell-like traits in NSCLC by protein phosphatase 1-mediated activation of Wnt/beta-catenin signaling. Cell Death Dis 9(10):942
- Milan M, Clemente-Ruiz M, Dekanty A, Muzzopappa M (2014) Aneuploidy and tumorigenesis in Drosophila. Semin Cell Dev Biol 28:110–115
- Ntziachristos P, Tsirigos A, Van Vlierberghe P, Nedjic J, Trimarchi T, Flaherty MS, Ferres-Marco D, da Ros V, Tang Z, Siegle J, Asp P, Hadler M, Rigo I, De Keersmaecker K, Patel J, Huynh T, Utro F, Poglio S, Samon JB, Paietta E, Racevskis J, Rowe JM, Rabadan R, Levine RL, Brown S, Pflumio F, Dominguez M, Ferrando A, Aifantis I (2012) Genetic inactivation of the polycomb repressive complex 2 in T cell acute lymphoblastic leukemia. Nat Med 18(2):298–301
- Pan MR, Peng G, Hung WC, Lin SY (2011) Monoubiquitination of H2AX protein regulates DNA damage response signaling. J Biol Chem 286(32):28599–28607
- Park KS, Qin L, Kabir M, Luo K, Dale B, Zhong Y, Kim A, Wang GG, Kaniskan HU, Jin J (2023) Targeted degradation of PRC1 components, BMI1 and RING1B, via a novel protein complex degrader strategy. Adv Sci (weinh) 10(10):e2205573
- Parreno V, Martinez AM, Cavalli G (2022) Mechanisms of Polycomb group protein function in cancer. Cell Res 32(3):231–253
- Parreno V, Loubiere V, Schuettengruber B, Fritsch L, Rawal CC, Erokhin M, Gyorffy B, Normanno D, Di Stefano M, Moreaux J, Butova NL, Chiolo I, Chetverina D, Martinez AM, Cavalli G (2024) Transient loss of Polycomb components induces an epigenetic cancer fate. Nature 629(8012):688–696
- Piunti A, Shilatifard A (2021) The roles of Polycomb repressive complexes in mammalian development and cancer. Nat Rev Mol Cell Biol 22(5):326–345
- de Potter B, Raas MWD, Seidl MF, Verrijzer CP, Snel B (2023) Uncoupled evolution of the Polycomb system and deep origin of non-canonical PRC1. Commun Biol 6(1):1144
- Ryu T, Spatola B, Delabaere L, Bowlin K, Hopp H, Kunitake R, Karpen GH, Chiolo I (2015) Heterochromatic breaks move to the nuclear periphery to continue recombinational repair. Nat Cell Biol 17(11):1401–1411
- Sad L, Mohamed DA, Elanwar NM, Elkady A (2021) CXCR4 and RIF1 overexpression induces resistance of epithelial ovarian cancer to cisplatin-based chemotherapy. J Cancer Res Ther 17(6):1454–1461
- Schuettengruber B, Bourbon HM, Di Croce L, Cavalli G (2017) Genome regulation by polycomb and trithorax: 70 years and counting. Cell 171(1):34–57
- Shcherbakova PV, Kunkel TA (1999) Mutator phenotypes conferred by MLH1 overexpression and by heterozygosity for mlh1 mutations. Mol Cell Biol 19(4):3177–3183
- Shukla S, Ying W, Gray F, Yao Y, Simes ML, Zhao Q, Miao H, Cho HJ, Gonzalez-Alonso P, Winkler A, Lund G, Purohit T, Kim E, Zhang X, Ray JM, He S, Nikolaidis C, Ndoj J, Wang J, Jaremko L, Jaremko M, Ryan RJH, Guzman ML, Grembecka J, Cierpicki T (2021) Small-molecule inhibitors targeting Polycomb repressive complex 1 RING domain. Nat Chem Biol 17(7):784–793
- Smogorzewska A, Matsuoka S, Vinciguerra P, McDonald ER 3rd, Hurov KE, Luo J, Ballif BA, Gygi SP, Hofmann K, D'Andrea AD, Elledge SJ (2007) Identification of the FANCI protein, a monoubiquitinated FANCD2 paralog required for DNA repair. Cell 129(2):289–301
- Sonobe R, Yang P, Suzuki MM, Shinjo K, Iijima K, Nishiyama N, Miyata K, Kataoka K, Kajiyama H, Kondo Y (2024) Long noncoding RNA TUG1 promotes cisplatin resistance in ovarian cancer via upregulation of DNA polymerase eta. Cancer Sci. https://doi.org/10.1111/cas.16150
- Staples CJ, Barone G, Myers KN, Ganesh A, Gibbs-Seymour I, Patil AA, Beveridge RD, Daye C, Beniston R, Maslen S, Ahel I, Skehel JM, Collis SJ (2016) MRNIP/C5orf45 interacts with the MRN

- complex and contributes to the DNA damage response. Cell Rep 16(10):2565-2575
- Su Y, Meador JA, Calaf GM, Proietti De-Santis L, Zhao Y, Bohr VA, Balajee AS (2010) Human RecQL4 helicase plays critical roles in prostate carcinogenesis. Cancer Res 70(22):9207–9217
- Tamburri S, Lavarone E, Fernandez-Perez D, Conway E, Zanotti M, Manganaro D, Pasini D (2020) Histone H2AK119 mono-ubiquitination is essential for polycomb-mediated transcriptional repression. Mol Cell 77(4):840–856
- Tomicic MT, Aasland D, Naumann SC, Meise R, Barckhausen C, Kaina B, Christmann M (2014) Translesion polymerase eta is upregulated by cancer therapeutics and confers anticancer drug resistance. Cancer Res 74(19):5585–5596
- Torres EM, Dephoure N, Panneerselvam A, Tucker CM, Whittaker CA, Gygi SP, Dunham MJ, Amon A (2010) Identification of aneuploidy-tolerating mutations. Cell 143(1):71–83
- Torres J, Monti R, Moore AL, Seimiya M, Jiang Y, Beerenwinkel N, Beisel C, Beira JV, Paro R (2018) A switch in transcription and cell fate governs the onset of an epigenetically-deregulated tumor in Drosophila. Elife
- Ui A, Nagaura Y, Yasui A (2015) Transcriptional elongation factor ENL phosphorylated by ATM recruits polycomb and switches off transcription for DSB repair. Mol Cell 58(3):468–482
- Varambally S, Dhanasekaran SM, Zhou M, Barrette TR, Kumar-Sinha C, Sanda MG, Ghosh D, Pienta KJ, Sewalt RG, Otte AP, Rubin MA, Chinnaiyan AM (2002) The polycomb group protein EZH2 is involved in progression of prostate cancer. Nature 419(6907):624–629
- Velasco A, Albert PS, Rosenberg H, Martinez C, Leach FS (2002) Clinicopathologic implications of hMSH2 gene expression and microsatellite instability in prostate cancer. Cancer Biol Ther 1(4):362–367
- Vissers JH, van Lohuizen M, Citterio E (2012) The emerging role of Polycomb repressors in the response to DNA damage. J Cell Sci 125(Pt 17):3939–3948
- Wagner VP, Webber LP, Salvadori G, Meurer L, Fonseca FP, Castilho RM, Squarize CH, Vargas PA, Martins MD (2016) Overexpression of MutSalpha complex proteins predicts poor prognosis in oral squamous cell carcinoma. Medicine (baltimore) 95(22):e3725
- Wang YL, Zhao WW, Bai SM, Feng LL, Bie SY, Gong L, Wang F, Wei MB, Feng WX, Pang XL, Qin CL, Yin XK, Wang YN, Zhou W, Wahl DR, Liu Q, Chen M, Hung MC, Wan XB (2022) MRNIP condensates promote DNA double-strand break sensing and end resection. Nat Commun 13(1):2638
- Wilczak W, Rashed S, Hube-Magg C, Kluth M, Simon R, Buscheck F, Clauditz TS, Grupp K, Minner S, Tsourlakis MC, Moller-Koop C, Graefen M, Adam M, Haese A, Wittmer C, Sauter G, Izbicki JR, Huland H, Schlomm T, Steurer S, Krech T, Lebok P (2017) Up-regulation of mismatch repair genes MSH6, PMS2 and MLH1 parallels development of genetic instability and is linked to tumor aggressiveness and early PSA recurrence in prostate cancer. Carcinogenesis 38(1):19–27
- Xu X, Chang CW, Li M, Liu C, Liu Y (2021) Molecular mechanisms of the RECQ4 pathogenic mutations. Front Mol Biosci 8:791194
- Yu S, Wang G, Shi Y, Xu H, Zheng Y, Chen Y (2020) MCMs in cancer: prognostic potential and mechanisms. Anal Cell Pathol (Amst) 2020:3750294
- Zeman MK, Cimprich KA (2014) Causes and consequences of replication stress. Nat Cell Biol 16(1):2–9
- Zhang XW, Sheng YP, Li Q, Qin W, Lu YW, Cheng YF, Liu BY, Zhang FC, Li J, Dimri GP, Guo WJ (2010) BMI1 and Mel-18 oppositely regulate carcinogenesis and progression of gastric cancer. Mol Cancer 9:40
- Zhou J, Zhang Y, Zou X, Kuai L, Wang L, Wang J, Shen F, Hu J, Zhang X, Huang Y, Chen Y (2020) Aberrantly expressed timeless regulates cell proliferation and cisplatin efficacy in cervical cancer. Hum Gene Ther 31(5–6):385–395



Zhou LZ, Xiao HQ, Chen J (2024) Mismatch repair gene MSH6 correlates with the prognosis, immune status and immune checkpoint inhibitors response of endometrial cancer. Front Immunol 15:1302797

**Publisher's Note** Springer Nature remains neutral with regard to jurisdictional claims in published maps and institutional affiliations.

